Nanoscale Optical Computing Using Resonance Energy Transfer Logic

Drawing on the nanometer-placement capabilities of self-assembly fabrication methods, the authors propose a new nanoscale device based on a single-molecule optical phenomenon called resonance energy transfer. This device enables a complete integrated technology, providing a potential path to molecular-scale computing. The authors present several important circuit elements, show how to compose these elements into computational nodes, and outline initial steps toward a prototype system.

Constantin Pistol
Chris Dwyer
Alvin R. Lebeck
Duke University

Nanoscale devices offer the possibility of a new era in computing. Device sizes at the molecular scale will let computer architects deploy a plethora of devices—creating, for example, million-core designs. Furthermore, because nanoscale devices could contain a significant amount of computational circuitry in an area smaller than a typical biological cell, they could prompt the emergence of new application domains.

To date, there is no clear winner in the field of nanotechnology for computing. CMOS continues its relentless march toward smaller feature sizes, but the cost of fabrication facilities increases with each new technology generation. Carbon nanotube and ring-gated nanorod field-effect transistors (FETs) are hopeful candidates, but obtaining control over the precise device length and achieving precise placement for arbitrary patterns remain open challenges.

This article proposes a new nanoscale technology for computing based on single-molecule optical devices called *chromophores.* In isolation, a given chromophore absorbs photons of a specific wavelength and emits photons at a different, lower-energy, wavelength. However, when appropriate chromophores are placed a few nanometers apart, the energy of an absorbed photon can be transferred to a neighboring chromophore through a process called *resonance energy transfer* (RET). This process provides the theoretical foundation for the creation of pass gates (both inverting and noninverting), using four chromophores per gate. These gates form a complete Boolean logic set, which we call *RET logic.*

A key requirement for RET logic is to place unique chromophores within a few nanometers of each other. Unfortunately, creating such devices using conventional top-down fabrication techniques is costly

0272-1732/08/$20.00 © 2008 IEEE Published by the IEEE Computer Society.

and extremely complex. Chemical self-assembly techniques, on the other hand, require less energy and time than placing individual atoms. Furthermore, self-assembly enables fabrication through composition and hierarchies. Different types of molecules can be fabricated independently using the most cost-effective method for each type. Larger molecular motifs can then be created through the composition of heterogeneous molecules.

We use DNA-based self-assembly as the fabrication method to place chromophores within specified distances. The specific DNA nanostructures we are fabricating in our lab are grids, in which we can place two pass gates and one wire crossover per grid vertex. The grids can be hierarchically assembled to create large arrays of pass gates—the nanoscale equivalent to sea-of-gates technology.

DNA-based self-assembly of chromophores provides a scalable, cost-effective technique for molecular-scale computing. However, the overall system must meet certain requirements to provide the appropriate abstractions for computing. These requirements include gates for nonlinear signal modulation, wires for linear signals, insulators, signal restoration, circuits with feedback, and I/O interfaces.

We show how to use RET logic on DNA grids to meet these requirements for a complete technology. Using this technology, we design and lay out several circuit elements (including a multiplexer and a decoder) and memory. These circuit elements can be used to design simple computational nodes targeted for specific application domains. The small size of individual nodes could enable biocompatible computing, in which an individual node could sense various activities (for example, the presence of certain proteins) within, or in samples taken from, a living organism.

From first principles, we construct analytic models for circuit performance and power consumption. These models show that RET logic can provide switching times on the order of nanoseconds while consuming only nanowatts per gate. In our sea-of-gates node, assuming 100 percent of the gates are consuming power, this bounds the power and energy at microwatts per node. Finally, we provide laboratory experimental results demonstrating initial steps toward a prototype system.

Molecular manufacturing: DNA self-assembly

DNA is an attractive substrate to investigate for applications in molecular-scale computing because it can form controlled, precise nanostructures. The binding rules that govern DNA self-assembly enable the creation of nanostructures with minimum pitch near a few nanometers. Furthermore, these nanostructures can organize active components with molecular-scale precision. Thus, DNA self-assembly is an enabling technology for a host of new computing paradigms.[1,2]

Double-stranded DNA is stable when the base pairs are *complementary*—that is, if A pairs with T, and G pairs with C. The central theme in applied self-assembly is to exert control over an otherwise spontaneous reaction to direct its outcome.[3] This control directs the assembly of materials into structures that are interesting and relevant to a given application. In the context of computer system fabrication, self-assembly can direct the formation of switching devices and wires to create logic circuitry, memory, and I/O interfaces. We can control the reaction by designing synthetic DNA strands to interact at specific temperatures (called melting temperatures) by carefully choosing their base sequences. Specifying the strand sequences can create a specific topology through base complementarity and the ability of DNA strands to fold (like tying a knot). Thus, sequence design is important because the interaction between strands must be thermodynamically favorable and result in a specific topology.[4]

Architects often create complex designs using a relatively small set of common building blocks, called motifs. DNA self-assembly can exploit this same design principle to hierarchically create more sophisticated, aperiodic structures. In the context of our RET logic, we focus on a grid-like structure. The grid can be *functionalized* (meaning that arbitrary single mol-

ecules can be attached) at several locations near each intersection in a fully *addressable* manner (meaning that each location is chemically distinct).

Hierarchical DNA self-assembly provides the fabrication characteristics—low cost and nanometer resolution—necessary for molecular-scale computation. However, the substrate must be complemented by suitable molecular-scale devices. RET provides the theoretical foundation for one potential class of devices that form a complete Boolean logic set.

RET logic

The molecularly precise fabrication enabled by DNA self-assembly can place and interconnect a limited number of components. At this scale, atoms and molecules must be counted as distinct components, and thus the fabrication of "bulk" electronic materials (greater than 1,000 atoms) is more challenging than the fabrication of single-molecule assemblies. For this reason, we are developing logic devices built from precisely placed collections of chromophores. The logic device we introduce here is built on principles from quantum mechanics and photochemistry, but is used here like a classical computational element. A useful analogy for our device is electronic current-mode logic, in which the current (high or low) through a circuit branch represents a Boolean value (1 or 0). However, the physical properties of the molecules in our device exhibit power dissipation and switching rates of the logic blocks that are fundamentally different from those in current-mode logic.

Resonance energy transfer

The theoretical basis for our logic technology is RET, which is the underlying mechanism that couples energy from a source (donor) chromophore to its destination (acceptor) chromophore. The transfer resembles the current rectification of a pn diode, because the excited-state energy of the donor transfers to the acceptor but not vice versa.

Figure 1 shows the transition energy diagram for this process. The donor (D) is first excited by the absorption of a photon with energy hv_1, denoted by D*. The excited-state donor energy, also called an *exciton,* is transferred to the acceptor (A), which becomes excited (A*) via RET and, through spontaneous decay of the excited state A* to A, emits a photon with lower energy hv_2. Förster first derived the latency of this process on the basis of classical charge dipole-dipole coupling and quantum mechanics; it is in the 10^{-11}-second to 10^{-9}-second time scale. Absorbed energy (labeled 1 in Figure 1) excites the donor from its ground state D_0 to D* and can decay radiatively (2) or nonradiatively (2a) to produce a photon (2b) through fluorescence RET. The energy of the acceptor excited state, A*, is always lower than the energy of the donor excited state, D*. Without additional energy, this constrains RET to a single direction: from donor to acceptor.

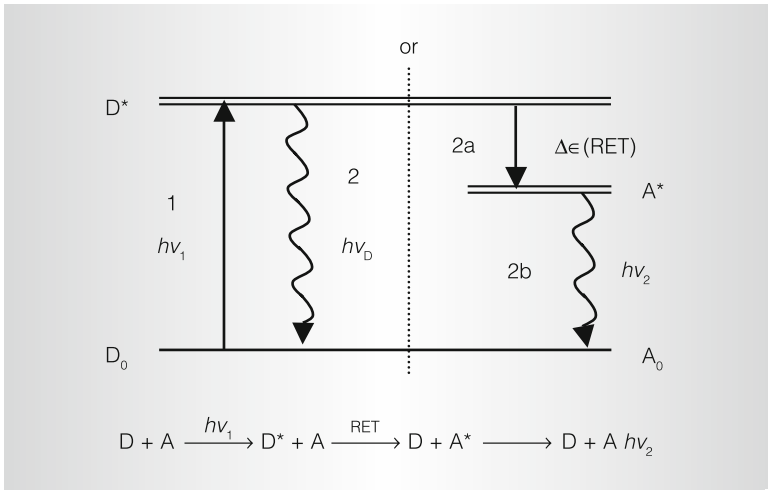

Figure 1. Transition energy diagram and expression for resonance energy transfer (RET). Absorbed energy (1) excites the donor from its ground state D_0 to D* and can decay radiatively (2) or nonradiatively (2a) to produce a photon (2b) through fluorescence RET.

Each chromophore has four (possibly unique) dipoles, two permanent and two transient. The permanent dipoles correspond to the ground state (μ_g) and the excited state (μ_e), and the transient dipoles represent the transitions between those two states: an absorption dipole (μ_{ab}) appears during the transition from the ground state to the excited state, and an emission dipole (μ_{em}) appears during the transition from the

Table 1. Parameters that impact RET efficiency.

Parameter	RET efficiency (Φ_T) scaling law	Description
Chromophore separation, r	$1/r^6$	Defined by relative placement of chromophores on a nanostructure
Spectral overlap, $J(\lambda)$	$J(\lambda)$	Property defined for pairs of chromophores derived from excitation and emission spectra; a measure of how well a donor couples to an acceptor
Förster radius, R_0	R_0^6	The separation to achieve 50% efficient RET
Relative orientation, κ	κ^2	Trigonometric relationship between chromophore dipoles

excited state back to the ground state. The transition from a μ_g to μ_e typically occurs in less than 10^{-15} s because of the purely electronic nature of this process.

The efficiency of RET between donor and acceptor defines the transfer rate, or latency, of an exciton passing through the system. This efficiency also defines important system-level properties such as power consumption, heat dissipation requirements, gain, and the signal-to-noise ratio. Four important parameters relate specific chromophore properties (and relative positions on a nanostructure) to RET efficiency. Table 1 identifies these parameters, which we can use to construct basic circuit elements.

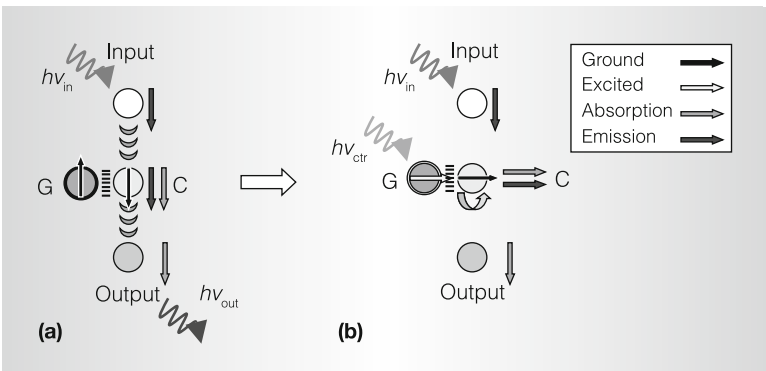

Figure 2. Schematic of inverting pass gate using RET in pass-mode (a) and ''high-Z'' mode (b). The gate (G), input, and output chromophores are rigidly bound to the substrate; the channel chromophore (C) can rotate in the pass-gate plane.

Gates

The relative orientation between chromophores (κ^2) is the key parameter that enables switching behavior. By forcing a chromophore's transient dipoles either into or out of alignment with neighboring chromophores, we can induce controlled pass-gate or inverting pass-gate switching behavior, respectively. To achieve this, we propose to exploit electrostatic interactions between chromophores.

The excited state of a nearby chromophore can realign a neighboring chromophore's ground-state dipole, thus changing the orientation of the chromophore's other dipoles. Careful design or selection of the chromophore, such that permanent and transient dipoles are parallel or perpendicular to the ground-state dipole, lets us control RET. Strong electrostatic interaction (alignment) has been demonstrated between the permanent dipoles of chromophores at close ranges (0.5 nm to 2 nm).[5]

Figure 2 shows our proposed design for an inverting RET pass gate that contains four chromophores. The input, output, and gate chromophores are rigidly bound to the substrate, and the channel chromophore is allowed to rotate in the gate plane. We control the degree of rotational freedom allowed for each chromophore through the specific choice of the molecule used to bind the chromophore to the substrate.[6] In an inverting pass gate, the channel's transitional dipoles are parallel to the ground state, whereas a noninverting pass gate has transitional dipoles that are perpendicular

to the ground state.[7] The gate chromophore has perpendicular permanent dipoles (μ_g, μ_e).

When the gate is not excited, the channel's μ_g aligns to the gate's μ_g through electrostatic interaction. The input and output chromophores are chosen to exhibit small μ_g to minimize the electrostatic interaction with the channel. With the channel and gate ground-state dipoles aligned, the channel's transitional dipoles (μ_{ab}, μ_{em}) also align with the input and output dipoles, enabling RET (Figure 2a). The pass gate is in pass mode. When the gate is excited, its dipole (μ_e) misaligns the channel to disrupt the RET cascade between the input and output, placing the pass gate in "high *Z*" mode (Figure 2b). In this mode the input signal does not propagate to the output.

Figure 3 illustrates how control over the relative angle of the channel chromophore influences input-to-output RET efficiency through the pass gate (Φ_T^2). The gate exhibits switching behavior over a range of chromophore separations and on/off ratios of 10^2 to 10^6. We expect the switching time of the channel to be about 100 ps, and the transfer time through the open gate to be defined by the rate of transfer from input to channel to output (about 200 ps to 2 ns).[7]

The pass gate (both inverting and noninverting) provides a complete logic family and is the fundamental component on which we build higher-level logic circuits. We are in the process of designing and optimizing the pass gate's configuration on our DNA substrate. Figure 4 shows how pass gates, together with wires, can be used to construct digital logic gates such as AND, OR, and NOT. With RET, we can create the equivalent of a wired-OR by selecting two input chromophores that have distinct excitation wavelengths but overlapping emission wavelengths, thus allowing both chromophores to undergo RET with a single output chromophore.

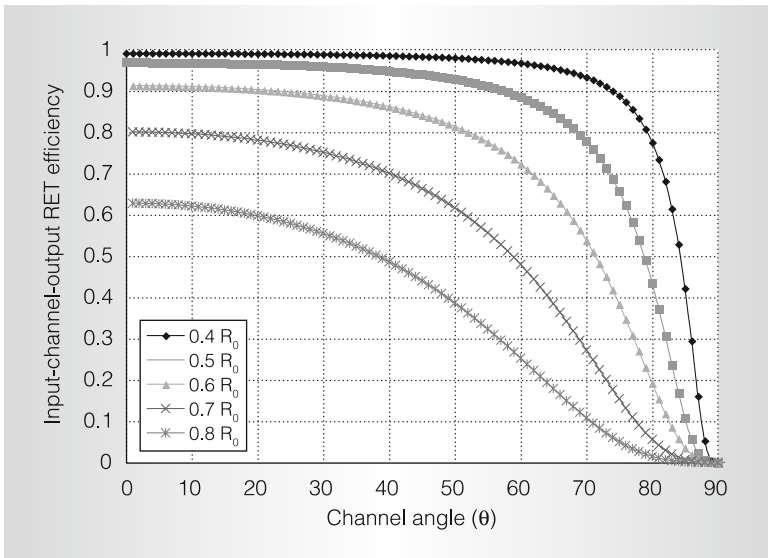

Figure 3. Plot of pass gate input-channel-output transfer efficiency versus channel chromophore angle (θ) for various input-channel-output separations (R_0 is the Förster radius; see Table 1). Channel angle θ is modulated by the gate chromophore.

Wires

To be useful for the transfer of information in circuits, RET must permit energy to transfer across long distances (tens of nanometers). One approach to creating wires is to use multiple different chromophores to form an energy cascade with multiple donor-acceptor steps. Researchers have demonstrated that 1D multichromophore cascades carry excited-state energy over distances of about 13 nm with greater than 90 percent efficiency on linear DNA.[8] Given that Φ_T is the per step transfer efficiency, a cascade of *n* chromophores will have a total efficiency of Φ_T^n, which scales poorly in the length of the cascade. Because of this, although a RET cascade can be used to implement wires, *energy migration* is potentially more efficient. EM occurs when the excited-state energy of a donor can diffuse within an ensemble of closely packed homogeneous donors with the same prob-

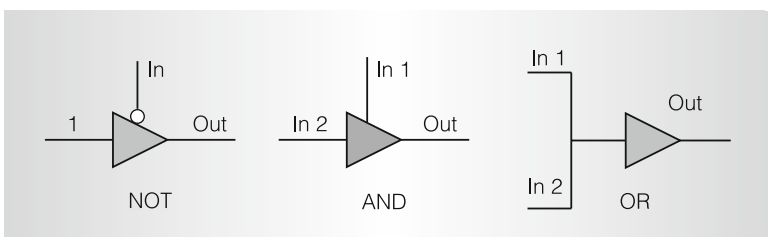

Figure 4. Schematic of AND, OR, and NOT gates using inverting and noninverting pass gates. The OR gate can be implemented as a wired-OR if signal restoration is not required.

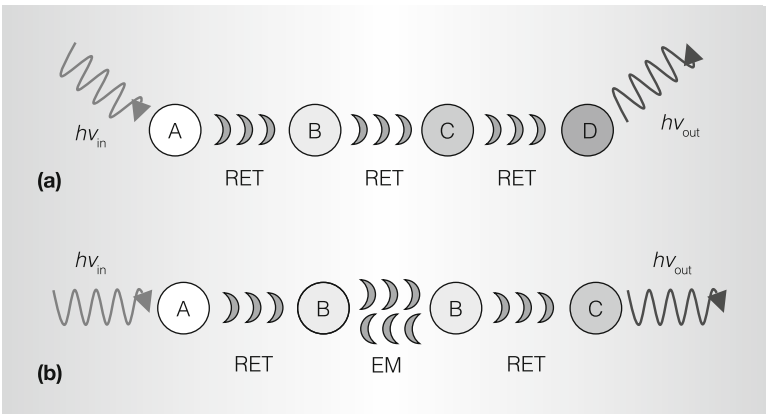

Figure 5. Schematic of a three-step RET cascade (a) and a RET-EM wire on a DNA grid (b). A photon with energy hv_{in} excites A and is transferred through the wire to C (or D), which emits a photon with energy hv_{out}.

ability of de-excitation as an individual donor. The implication is that EM along arrays of identical chromophores can extend the distances over which RET can take place well beyond the limits of the Förster radius. The observed time scale for EM is about 10^{-12} s per transfer step, which is faster than RET but nondirectional.

Figure 5a illustrates a possible 2D energy transfer wire. Chromophore A (the donor) can be excited by a photon from the far field and, through RET, directionally couple the energy to B, then to C, then D, and ultimately to an emitted photon with energy hv_{out} (of lower energy due to the Stokes shift effect). Figure 5b shows an example of a hybrid RET-EM wire. The first chromophore pair, A-B, is a RET pair that couples energy into a series of EM-coupled chromophores. The output is another RET pair, B-C.

A wire of length L nm is expected to have a transfer time of approximately L/r ps (for EM), and 10 L/r ps (for RET), for r-nm chromophore spacing, where r is far less than the Förster radius, R_0. For wires, the design goal is to minimize r and maximize $J(\lambda)$ and κ^2 within the constraints imposed by the substrate. The critical substrate requirement is the capability to place chromophores (single molecules) at a pitch of $r = 1$ nm to 3 nm pitch, a constraint easily met with DNA nanostructures. In addition, spectrally distinct RET or EM wires can cross within close proximity to facilitate nonplanar circuits.

Integrated RET technology

Although the pass gates are logically complete, implementing larger logical circuits creates challenges with efficient insulation, the power supply, feedback, memory, and macroscale I/O interfaces.

Insulators

A critical aspect of any dense computational technology is the prevention of signal interference between independent devices and wires. In conventional CMOS, oxide and minimum physical separation are used to prevent crosstalk, which in our technology is unintentional RET. Our system can employ a similar physical separation by placing molecules at fixed distances from one another. Specifically, because RET degrades as $1/r^6$, the coupling between independent RET wires can be reduced to about $1/X^6$ by a separation of $X \times R_0$, or 10^{-7} when $X = 10$. Wavelength multiplexing at the device level is another way to achieve greater device and wire density per wavelength layer. Devices in a given layer must be separated to prevent crosstalk, but they can be nearby devices in other layers without penalty.

Signal restoration: Energy supply and feedback

Each step along a RET cascade is energetically downhill. That is, the end of a cascade (long wavelength) cannot couple to the beginning of a cascade (short wavelength) without additional energy. However, a complete technology requires feedback from outputs to inputs to implement cross-coupled logic gates or finite-state machines. We can use the pass gates we presented earlier to provide signal restoration by inserting NOT gates at the output of each logic module. The constant input to the NOT gate can pass through the buffer, and it suffers only one loss due to RET.

Signal restoration from long wavelengths (low energy) to short wavelengths (high energy) requires additional energy. The proposed pass gates can provide this functionality if the input 1 to the pass gate is generated from an external far-field optical source called an optical pump (conceptually analogous to V_{DD}), and the gate is controlled by the signal to either

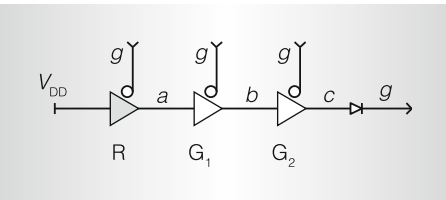

Figure 6. Set of RET gates including restoration gate R for feedback and energy supply. Each EM wire is annotated with its exciton frequency band. V_{DD} is the optical pump frequency.

invert or pass. Such gates restore both the frequency and the intensity of excitons in a single device. Importantly, because V_{DD} is a far-field signal, it does not need to be routed.

Figure 6 shows a set of inverting pass gates that includes a restoration gate for energy supply and feedback. Each EM wire is annotated with its excitation frequency band; V_{DD} is the optical pump frequency, and $V_{DD} > a > b > c > g$. In this example, the gate inputs of R, G_1, and G_2 use the same frequency g, although this is not required. In each case, the gate input frequency must be distinct from the source and drain frequencies. Higher frequencies can be converted to lower frequencies in the wire using RET cascades that act as down-converting diodes.

An alternative method for signal restoration is to use an external supply that blankets the system with infrared photons of the necessary energy to amplify the excitation of a given chromophore and thus excite it *energetically backward* to an adjacent chromophore.[9] The specific energy of the IR photons depends on the detailed band structure of the two chromophores, but in principle should be in the near- to mid-IR range to achieve an 8× to 10× gain.

Memory cells

With the ability to restore signals and create circuits with feedback, we can create the D latch in Figure 7a. Wires are annotated with excitation frequency (*a, b, c, g, d*). To minimize the gate set complexity, we assume all restoring gates (dark gray) have the same output frequency *a*.

Compared with a standard CMOS design, this design needs additional pass gates to enable 0-to-1 transitions, because the logical zero output of a pass gate does not have pull-down capability.

Gates are attached to the DNA grid substrate at the interface between tile arms, and wires can cross on tile centers. Assuming a half-pitch size L, with each tile having length and width $2L$, the minimum separation is $L\sqrt{2}$.

With our current DNA substrate, L is 10 nm, and the D latch size is 20 nm × 40 nm. Figure 7b shows a more complex 40 nm × 60 nm SRAM (synchronous RAM) memory cell that can be used for memory arrays. Signal restoration on directional cell inputs and outputs can be added on the shared connection points between cells.

Decoders, multiplexers, and adders

Figure 8a shows the layout of a four-way multiplexer, and Figure 8b shows a 2/4 decoder with enable input. Each of these devices measures 40 nm × 60 nm. Figure 8c shows a 40 nm × 40 nm 1-bit full adder cell for arithmetic units.

Macroscale I/O interfaces

Energy transfer logic does not necessarily require direct addressing of individual components. Input signals can be sent into the system and absorbed by any (or all) input chromophores simultaneously. Similarly, output chromophores can be observed by ensemble measurements. This method requires strict wavelength division multiplexing on the inputs, the internal RET wires, and the output chromophores to disambiguate control and output signals. The design challenge is to find instances of chromophores (that is, real molecular structures) that can satisfy the wavelength and spectral overlap requirements for inputs, wires, gates, and outputs.

Analysis

To estimate the switching speed and power dissipation of circuits based on RET logic, we start from a simple configuration consisting of two pass gates (A and B) connected by an EM wire (see Figure 9).

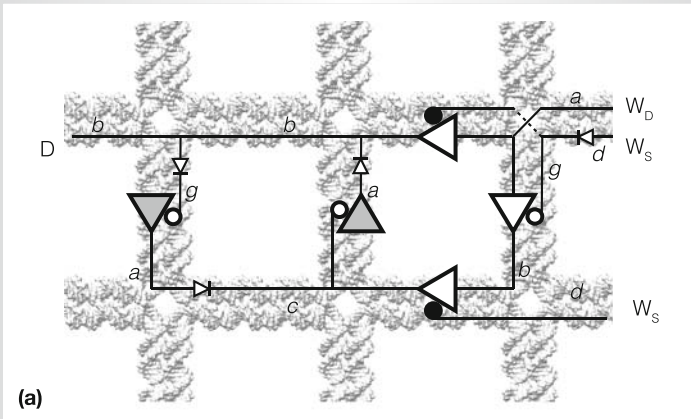

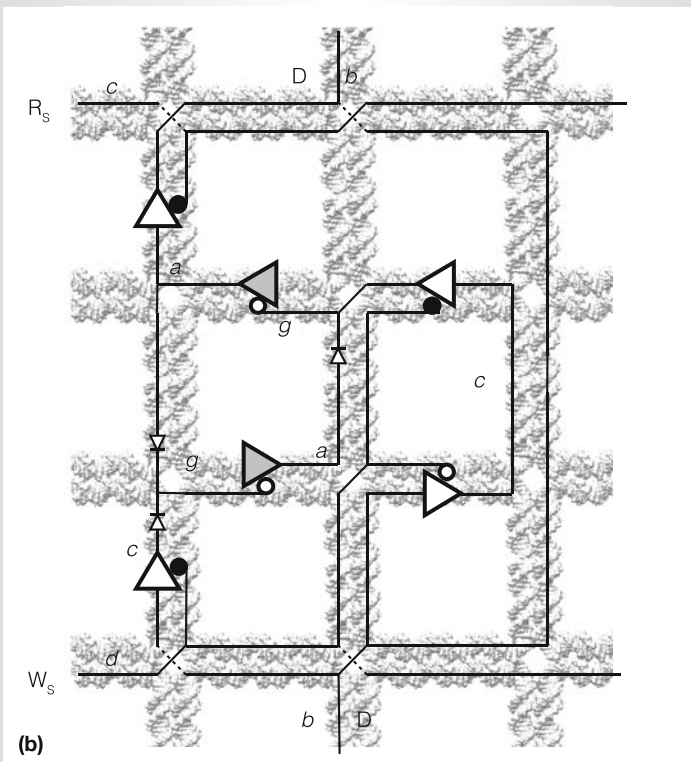

Figure 7. Memory latch, 20 nm × 40 nm (a), and memory cell, 40 nm × 60 nm (b). R_S and W_S are read and write select lines, and D is the data line.

The input to the source of gate A has rate k_{in} and frequency v_{in}. After passing through gate A and through the wire, the rate and frequency at the gate input of B are k_g and v_g and respectively. We consider that with the line asserted (logical 1), k_g must be at least $1/\tau_{G\_ex}$ to maintain G in its excited state and gate B in its switched configuration. Given m RET steps (3 in this case) and an EM wire of length l, the minimal necessary input rate is

$$k_{\text{inmin}} \approx \frac{\alpha l k_w + k_g}{\Phi_P}$$

where Φ_P is the overall transfer efficiency of the path. The EM wire can hold up to l excitons; we assume that it must hold at least a fraction α to sustain rate k_g at the output. The circuits we described earlier show gate-to-gate wire lengths ranging from 10 nm to 30 nm; for this analysis, we assume l to be 20. We use this simple model to derive order-of-magnitude estimations for RET logic switching time and power dissipation.

Table 2 shows the estimated characteristics of a single gate-wire-gate path. Given the calculated ~70 percent transfer efficiency, we estimate the necessary input excitation rate at 8.4 GHz, and the switching time is approximately 2 ns. The length of the EM wire has a significant impact on dissipated power and must be considered when optimizing circuit layouts. Given a high gating factor, most power is dissipated when the path is in the asserted state with the input gate in pass mode. The two main sources of thermally dissipated energy are the Stokes shift (down frequency) inherent in each RET step and non-RET induced de-excitation. A significant fraction of the latter is generally not thermalized but emitted as far-field fluorescence photons.

Table 3 shows the estimated power consumption of a node of 150 × 150 tiles with 22,500 restoring gate-wire-gate paths to be in the μW range. A node of this size can implement a basic computational device.

Application domains

Given the circuit elements we have described, it is possible to construct a simple computational node on a single large DNA grid. Although large periodic DNA structures have been demonstrated, we assume the size of aperiodic structures is limited to 150 × 150 cruciform tiles, or a total of 22,500 tiles. Given our mapping of

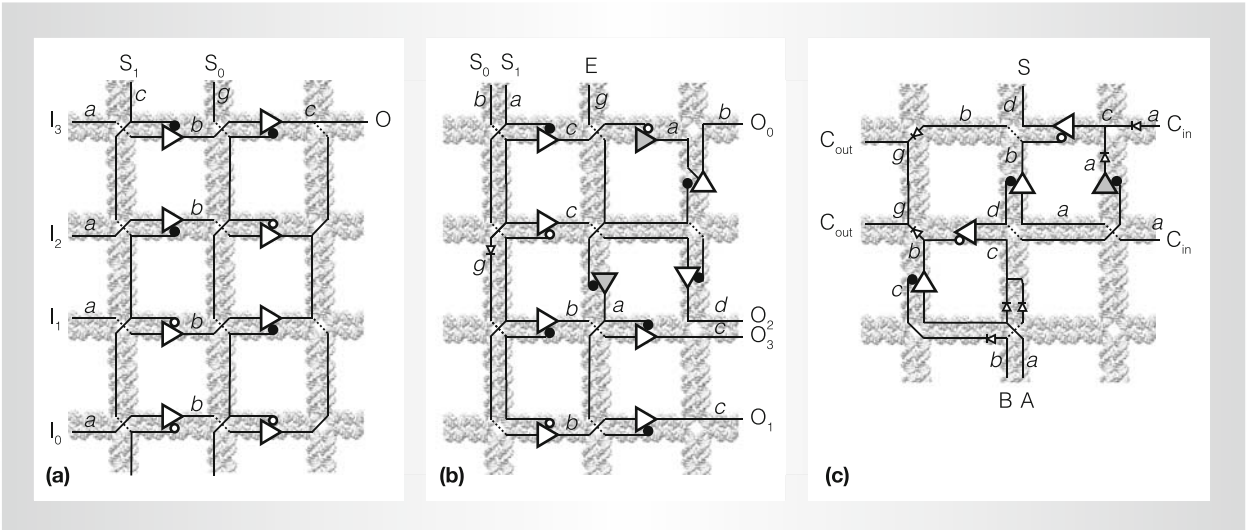

Figure 8. Four-way multiplexer, 40 nm × 60 nm (a), 2-to-4 decoder, 40 nm × 60 nm (b), and one-bit full adder, 40 nm × 40 nm. S1 and S0 are select lines, E is the enable input, C_{in} and C_{out} are adder carry-in and carry-out respectively.

two primitive logic gates per tile, we have 45,000 total gates per node. This is twice as many as in previously proposed DNA self-assembled carbon nanotube designs.[10]

We are in the early stages of floorplanning a node, but we believe that a node can contain an 8-bit microcontroller accumulator-based CPU core and 128 bytes of memory. This would dedicate slightly more than half the area to memory. The remaining area would be used to implement a simple instruction set architecture such as the STMicroelectronics ST6 or the Freescale Semiconductor RSO8 (see http://www.datasheetcatalog.com/stmicroelectronics/498 and http://www.freescale.com/files/microcontrollers/doc/data_sheet/MC9RS08KA2.pdf).

Nanoscale sensing

RET can be used to sense a variety of chemical compounds and environmental conditions. For example, there are fluorescence RET sensors for organic and inorganic compounds, pH, viruses, temperature changes, proteins, DNA, RNA, and so on.

There are various ways of augmenting our node to support protein sensing. Here, we explore two. First, the protein sensors could be memory mapped. In this scenario, predetermined memory addresses are set aside for access to sensed values via load instructions. The second method exploits the biological compatibility of our entire system. Because RET is the method used for sensing and computing, we can directly integrate the sensing mechanisms into the system design.

There may be many ways to exploit an integrated design methodology, but in this article we examine methods for sensing to directly modify instructions. Specifically, certain SRAM cells can be augmented with appropriate sensing mechanisms that force the memory location to the value 1 or 0, as needed. These environmentally modified memory locations can be designed to correspond to specific instruction bits. For example, an ADD opcode could be modified into a SUB opcode. Similarly, instruc-

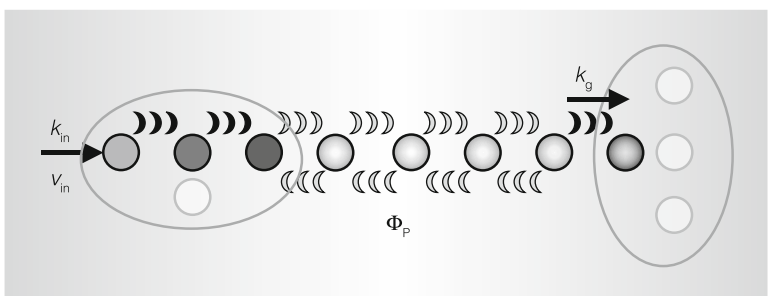

Figure 9. Latency and power dissipation analysis: The drain output of one pass gate connects to the gate input of another pass gate through an EM wire.

Table 2. RET path model.

Parameter	Description	Nominal values
τ_{rot}	Rotational correlation time of channel	10 ps
τ_{G_ex}, k_g	Excited lifetime and rate of gate	1 ns, 1 GHz
τ_{W_ex}, k_w	Excited lifetime and rate of a single EM chromophore	2 ns, 0.5 GHz
Φ_{RET}, τ_{RET}	Efficiency and time for RET step	0.9, 100 ps
Φ_{EM}, τ_{EM}	Efficiency and time for EM step	0.999, 1 ps
m	Number of RET steps	3
l	Number of EM steps	20
α	Fraction of excited EM chromophores in wire necessary to sustain k_g at the output	0.5
$\Phi_P = \Phi_{RET}{}^m \Phi_{EM}{}^l$	Input to gate path efficiency	0.71
$k_{in\_min} \approx (\alpha l k_w + k_g)/\Phi_P$	Input excitation rate that generates k_g	8.4 GHz
$t_{l\_prop} \approx \alpha l / k_{in} \Phi_P + \tau_{rot}$	Transition time for low to high	1.8 ns
$t_{0\_prop} \approx \tau_{W\_ex} + \tau_{rot}$	Transition time for high to low	2.1 ns

tion operands could be modified by the sensing mechanism to change a shift amount or a branch target.

The primary motivation for directly modifying instructions is improved code density. With only 128 bytes of memory available, judicious use of instructions is paramount to providing sufficient computational abilities. The simple task of querying a sensor to determine if a specific protein is present can require several bytes of instruction memory to load a value and compare it for branching. Instead, a single one-byte branch instruction could be used that changes to a no operation (NOP) and escape when the protein binds. We are exploring this unique opportunity for instruction set design and encoding.

The long-term vision is that an integrated sensor could be custom designed and fabricated (at low cost) to provide appropriate sensing needs for molecular-scale biological applications. However, some applications might require greater computational abilities than what is available on a single node. Thus, next we outline a proposed method for individual nodes to collaborate to solve larger computational problems.

Diffusion-limited computation

RET forms the basis for both computation and sensing in our proposed systems. It also integrates nicely with techniques for external communication: input through excitation at specific wavelengths, and output by emission at specific wavelengths. These same mechanisms can provide communication between nodes suspended in an aqueous solution. At sufficiently high concentrations, nodes would come into physical contact with one another periodically and exchange information. The period between contacts is determined by the

Table 3. Estimated node power consumption.

Term	Definition	Value
N	No. of restoring gates connected to pump	22,500
f_{th}	Ratio of radiative to nonradiative (thermalized) excitation loss	0.1
$P_{1\_Stokes} \approx N[k_g h(v_{in} - v_{out}) + \alpha l k_w h(v_{in} - v_{wire})]$	Power thermalized on all N gates due to Stokes shift in ''1'' state (600-nm input, 625-nm wire, 650-nm output)	2.1 μW
$P_{1\_th} \approx N k_{in\_min} f_{th} h v_{in} + P_{1\_Stokes}$	Power thermalized in ''1''	8.31 μW
$P_{0\_th} \approx N[k_{in\_min} f_{th}(1 - \Phi_P) h v_{in} + k_{in\_min} \Phi_P h(v_{in} - v_{wire})]$	Power thermalized in ''0-1''	1.8 μW
$P_{10\_th} \approx N \alpha l k_w f_{th} h v_{wire}$	Power thermalized in ''1-0''	3.6 μW

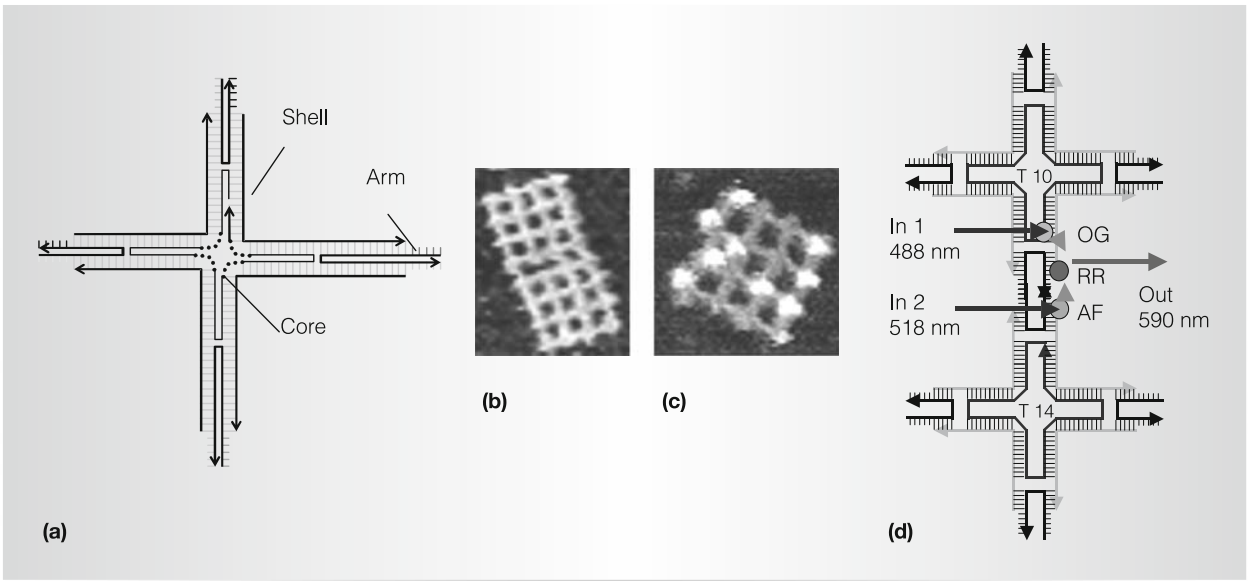

Figure 10. Schematic of a cruciform motif (a), an 8 × 4 grid (b), a protein-patterned grid (c), and schematic of the OR gate (d). (OG: input chromophore Oregon Green; AF: input chromophore Alexa Fluor 535; RR: output chromophore Rhodamine Red.)

concentration and diffusion rates of the nodes—thus the term *diffusion-limited computation.*

Diffusion-limited computation could be used to compute the average binding rate of a set of proteins or small molecules such as messenger RNA (mRNA). Information about the binding rate can be used to infer local concentrations of these molecules, which are important markers of bioactivity and cellular health.[11] The challenge is to perform this averaging at the nanoscale over a large set of possible proteins (for example, about 4×10^5 unique proteins can be found in any individual human cell). A distributed set of nodes, each designed to detect a subset of the total protein set, could employ diffusion to sample and average protein concentrations over a large observation window to track overall protein expression.

The period of time between node interactions (diffusion time) is proportional to $<X> \times D^{-1}$, where $<X>$ is the average node-node separation, and D is the diffusion constant of a node. For the nodes to successfully collaborate on larger problems, it is important to balance the size of the node (that is, D), the concentration of nodes (that is, $<X>$), and the available memory for computation between interactions.

Toward a prototype

We turn now to our initial results in working toward molecular-scale computing. The purpose of the experiment we report here is twofold: to show that the DNA grid lets us place chromophores sufficiently close to achieve RET interaction, and to demonstrate simple wired-OR RET behavior.

Figure 10a shows the cruciform motif we use to build the DNA grid. The motif consists of three smaller motifs: a core, four shells, and four arms. Figure 10 also shows an atomic force microscope image of a hierarchically built 8 × 4 grid (Figure 10b) and a protein-patterned nanostructure (Figure 10c), each developed in our laboratory using methods that we and our colleagues describe in another publication.[12]

Using chemistry similar to that used to attach proteins, it is possible to attach chromophores to specific sites on the DNA grid. The available sites on each grid occur at the intersection between motifs and at the center of the cruciform motif. The spacing between sites at the motif intersections is about 1.3 nm, and about 20 nm between motif centers. The wired-OR gate is assembled using three chromophores (fluorescent dyes)—two for the input signals (Oregon Green and Alexa Fluor 535),

Table 4. Observed RET output from the OR gate under 488-nm and 518-nm excitation.

Input 1: 488 nm	Input 2: 518 nm	RET output: 590 nm (optical fluorescence counts)
Off	Off	0
On	Off	39
Off	On	31
On	On	70

and one for the output signal (Rhodamine Red)—attached to the grid as shown in Figure 10d. The two inputs are excited by wavelengths of light at 488 nm for Oregon Green, and 518 nm for Alexa Fluor 535. The input chromophores undergo RET with the Rhodamine Red output chromophore, which has an emission peak at 590 nm.

We experimentally assemble scaffolds with the attached OR gates as just described. A fluorometer measures the output of the assembly in the 300-nm to 800-nm range under various input conditions. A custom dual-beam excitation source generates excitation. We estimate that the sample contains about 1,012 gates; Table 4 shows the output for excitation of 488 nm (In 1), 518 nm (In 2), and simultaneous 488 nm and 518 nm (In 1 + In 2). We isolate the specific contribution of the output (Rhodamine Red) chromophore due to RET from the background fluorescence by subtracting the normalized readout of a baseline grid assembly with the same chromophores placed at distances much greater than their respective Förster radii (thereby preventing RET).

These results demonstrate the capability to place three chromophores sufficiently close to transfer excited-state energy from two distinct inputs to the same output, as in an OR gate.

Nanoscale computing could open new areas of exploration, such as biologically compatible computation. The RET logic we've described presents one possible path toward a molecular-scale computing substrate. The densities achievable on existing DNA nanostructures result in a D latch occupying 20 nm × 40 nm, a complete SRAM cell occupying 40 nm × 60 nm, and a full adder occupying 40 nm × 40 nm. New nanostructures could further improve densities. Although our DNA nanostructures and chromophore-based wired-OR gate constitute only a first step toward nanoscale computing, they demonstrate the ability to precisely control single-molecule placement and to interface with the devices at the macroscale. We are currently exploring the fabrication of the inverting and noninverting pass gates we've proposed in this article. MICRO

Acknowledgments

This work is supported in part by the National Science Foundation (CCF-0829911 and CCF-0702434).

References

1. C. Pistol and C. Dwyer, ''Scalable, Low-Cost, Hierarchical Assembly of Programmable DNA Nanostructures,'' *Nanotechnology*, vol. 18, no. 12, Mar. 2007, pp. 125305-125309.
2. P.W.K. Rothemund, ''Folding DNA to Create Nanoscale Shapes and Patterns,'' *Nature*, vol. 440, no. 7082, 16 Mar. 2006, pp. 297-302.
3. G.M. Whitesides and B.A. Grzybowski, ''Self-Assembly at All Scales,'' *Science*, vol. 295, Mar. 2002, pp. 2418-2421.
4. C. Pistol, A.R. Lebeck, and C. Dwyer, ''Design Automation for DNA Self-Assembled Nanostructures,'' *Proc. 43rd Design Automation Conf.* (DAC 06), ACM Press, 2006, pp. 919-924.
5. A.W. Harper et al., ''Translating Microscopic Optical Nonlinearity into Macroscopic Optical Nonlinearity: The Role of Chromophore-Chromophore Electrostatic Interactions,'' *J. Optical Soc. of America B*—

Optical Physics, vol. 15, no. 1, Jan. 1998, pp. 329-337.
6. J. Shi and D.E. Bergstrom, ''Assembly of Novel DNA Cycles with Rigid Tetrahedral Linkers,'' *Angewandte Chemie, Int'l Edition*, vol. 36, no. 1-2, Feb. 1997, pp. 111-113.
7. J.R. Lakowicz, *Principles of Fluorescence Spectroscopy*, Kluwer Academic/Plenum Publishers, 1999.
8. Y. Ohya et al., ''Multistep Fluorescence Resonance Energy Transfer in Sequential Chromophore Array Constructed on Oligo-DNA Assemblies,'' *Bioconjugate Chemistry*, vol. 14, no. 6, Nov. 2003, pp. 1057-1066.
9. D.W. Brousmiche et al., ''Fluorescence Resonance Energy Transfer in a Novel Two-Photon Absorbing System,'' *J. American Chemical Soc.*, vol. 125, no. 6, 12 Feb. 2003, pp. 1448-1449.
10. J.P. Patwardhan et al., ''A Defect Tolerant Self-Organizing Nanoscale SIMD Architecture,'' *Proc. 12th Int'l Conf. Architectural Support for Programming Languages and Operating Systems* (ASPLOS 06), ACM Press, 2006, pp. 241-251.
11. A.P. Arkin and D.A. Fletcher, ''Fast, Cheap and Somewhat in Control,'' *Genome Biology*, vol. 7, no. 8, 2006, pp. 114.1-114.6.
12. S.H. Park et al., ''Finite-Size, Fully-Addressable DNA Tile Lattices Formed by Hierarchical Assembly Procedures,'' *Angewandte Chemie*, vol. 45, no. 40, 2006, pp. 735-739.

Constantin Pistol is a doctoral student in computer science at Duke University. His research interests include architectures and digital-circuit design for molecular-scale computing systems. He has a BS in computer science from University of Craiova, Romania, and an MS in computer science from Duke University.

Chris Dwyer is currently an assistant professor of electrical and computer engineering and of computer science at Duke University. His research interests include self-assembly, DNA, and the development of circuit technologies for molecular-scale fabrication processes. He has a BS in computer engineering from Pennsylvania Sate University, University Park, and an MS and a PhD in computer science from the University of North Carolina at Chapel Hill.

Alvin R. Lebeck is a professor of computer science and of electrical and computer engineering at Duke University. His research interests include architectures for emerging nanotechnologies and memory systems. He has a PhD in computer science from the University of Wisconsin–Madison. He is a senior member of the IEEE and a member of the ACM.

Direct questions and comments about this article to Chris Dwyer, Duke University, 130 Hudson Hall, Box 90921, Durham, NC 27708; dwyer@ece.duke.edu.